Modification of Hematite Electronic Properties with Trimethyl Aluminum to Enhance the Efficiency of Photoelectrodes

ARTICLE *in* JOURNAL OF PHYSICAL CHEMISTRY LETTERS · OCTOBER 2014

Impact Factor: 7.46 · DOI: 10.1021/jz501751w

10 AUTHORS, INCLUDING:

Massimo Tallarida
Cells Alba
58 PUBLICATIONS **476** CITATIONS
SEE PROFILE

Chitta Das
Brandenburg University of Technology Cott…
7 PUBLICATIONS **48** CITATIONS
SEE PROFILE

Aile Tamm
University of Tartu
26 PUBLICATIONS **114** CITATIONS
SEE PROFILE

Markku Leskelä
University of Helsinki
783 PUBLICATIONS **18,158** CITATIONS
SEE PROFILE

THE JOURNAL OF PHYSICAL CHEMISTRY Letters

Letter

pubs.acs.org/JPCL

Modification of Hematite Electronic Properties with Trimethyl Aluminum to Enhance the Efficiency of Photoelectrodes

Massimo Tallarida,*[,†] Chittaranjan Das,[†] Dejan Cibrev,[‡] Kaupo Kukli,[§,∥] Aile Tamm,[∥] Mikko Ritala,[§] Teresa Lana-Villarreal,[‡] Roberto Gómez,[‡] Markku Leskelä,[§] and Dieter Schmeisser[†]

[†]Applied Physics—Sensors, Brandenburg University of Technology, Konrad Wachsmann Allee, 17, 03046, Cottbus, Germany

[‡]Institut Universitari d'Electroquímica i Departament de Química Física, Universitat d'Alacant, Apartat 99, E-03080 Alicante, Spain

[§]Department of Chemistry, University of Helsinki, P.O. Box 55, FI-00014, Helsinki, Finland

[∥]Institute of Physics, University of Tartu, Ravila 14c, 50411 Tartu, Estonia

Supporting Information

ABSTRACT: The electronic properties of hematite were investigated by means of synchrotron radiation photoemission (SR-PES) and X-ray absorption spectroscopy (XAS). Hematite samples were exposed to trimethyl aluminum (TMA) pulses, a widely used Al-precursor for the atomic layer deposition (ALD) of Al_2O_3. SR-PES and XAS showed that the electronic properties of hematite were modified by the interaction with TMA. In particular, the hybridization of O 2p states with Fe 3d and Fe 4s4p changed upon TMA pulses due to electron inclusion as polarons. The change of hybridization correlates with an enhancement of the photocurrent density due to water oxidation for the hematite electrodes. Such an enhancement has been associated with an improvement in charge carrier transport. Our findings open new perspectives for the understanding and utilization of electrode modifications by very thin ALD films and show that the interactions between metal precursors and substrates seem to be important factors in defining their electronic and photoelectrocatalytic properties.

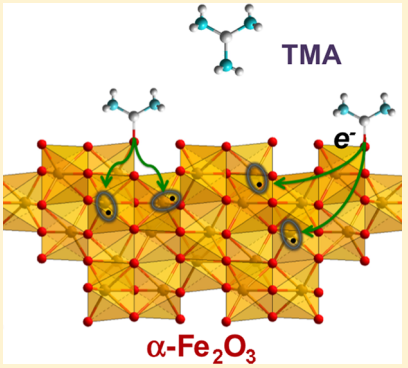

SECTION: Physical Processes in Nanomaterials and Nanostructures

Hematite (α-Fe_2O_3) is a functional material for many applications, ranging from sensors[1] to photovoltaics[2] and photoelectrochemical (PEC) water splitting.[3] For an efficient use of α-Fe_2O_3 for water splitting, many issues need to be solved, included a low absorption coefficient, short charge carrier diffusion length, and strong carrier recombination. In addition, because of the energy location of the conduction band edge, water splitting PEC cells based on hematite require the application of external bias.[3]

Hematite is a strongly correlated material with many poorly understood properties. For example, the mechanism of charge carrier conduction is still debated.[4] For electrons it is preferentially described with the small polaron model: electrons hop between neighboring Fe^{3+} atoms with the creation of local Fe^{2+} species[4−6] and are expected to self-trap.[6] Thus, both bulk and surface electronic properties are important for PEC water splitting with hematite photoanodes.[7,8]

Recently, it was demonstrated that one layer of Al_2O_3 grown by atomic layer deposition (ALD) with trimethyl aluminum (TMA) and water on α-Fe_2O_3 decreases the onset potential by about 100 mV.[9] This effect was attributed to the passivation of surface states and the consequent decrease of photocarrier recombination,[9] although the surface passivation mechanism was not directly studied.[9,10] Other methods were developed to increase the photoresponse.[11−13]

Some of us have demonstrated that the Al-precursor for the ALD of Al_2O_3 (TMA) reacts strongly with oxide substrates, eventually producing reduced species in the interfacial region.[14,15] We will show in this Letter the occurrence of a novel effect as a consequence of the reactions between TMA and hematite, that is, electron doping of α-Fe_2O_3 and, depending on the nature of hematite, Fe^{3+} to Fe^{2+} partial reduction. The electron doping is supposed to have a polaronic nature, that is, it is associated with small local structural distortions,[4] causing a change in the hybridization of O 2p with Fe 3d and Fe 4s4p states in hematite. We will also show that the TMA modified hematite electrodes show a strong increase of PEC efficiency. Obviously, electron doping is compatible with the strong PEC enhancement.

In this study, we used three different hematite photoabsorbers: two planar samples made by ALD on Si (sample A and B, with thickness values of 70 nm) using two different Fe precursors (dimethylaminomethyl-ferrocene, $CpFeC_5H_4CHN(CH_3)_2$, and ferrocene, $Fe(C_5H_5)_2$) and ozone, and a nanostructured sample made by growing hematite nanocolumns prepared by chemical bath deposition on fluorine-doped tin oxide (F:SnO_2, FTO) (sample C, with a thickness of

Received: August 19, 2014
Accepted: October 3, 2014

   dx.doi.org/10.1021/jz501751w | J. Phys. Chem. Lett. 2014, 5, 3582−3587

400 nm) to show that the origin of the photoresponse enhancement does not depend on either the way hematite was synthesized or the substrate that was used (see Supporting Information SI0, for details of the experimental methods).

This Letter is organized as follows: (i) PES characterization of hematite before and after TMA modification; (ii) XAS characterization of hematite before and after TMA modification; (iii) discussion of the possible reasons for the observed spectroscopic changes; (iv) consideration of the different behavior of samples B and C in PES; (v) details of the valence band (VB) to demonstrate the absence of reduction from Fe^{3+} to Fe^{2+} in sample C; (vi) PEC characterization to show that TMA modified hematite photoelectrodes show enhanced photoresponse.

The VB of Fe_2O_3 is characterized by three main features within the binding energy range of 2−10 eV. In the literature, peak **a** was attributed to O 2p−Fe 3d hybridized states,[16] whereas a mixed O 2p and O 2p−Fe 4s4p character was assigned to the two broader features **b** and **c**.[16,17] Instead, the broader feature **s** at higher binding energy was assigned to a satellite emission due to final state effects.[18,19] As such, its presence is related with peak **a** as the satellite **s** is assigned, within the context of configuration interaction model, to unscreened Fe $3d^4$ final states and peak **a** to screened Fe $3d^5\underline{L}$ final states,[18,19] being originated by the same initial state. Along with these typical states, an extra peak **d** at low binding energy is also observed in sample A. A similar feature above the VBM of hematite was assigned to Fe^{2+} species.[20]

After just one pulse of TMA at 250 °C, the shape of the VB spectrum in Figure 1a changes drastically, with a decrease of

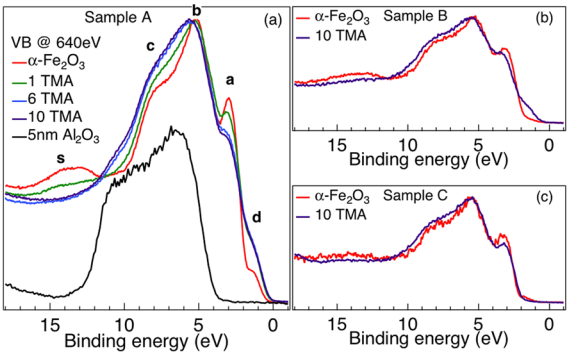

Figure 1. (a) Valence band (VB) spectra of sample A before and after the TMA pulses measured with 640 eV photons. Peak **a** is assigned to O 2p−Fe 3d hybridized states and peaks **b** and **c** to O 2p lone pair and O 2p−Fe 4s4p hybridized states. Feature **s** is related to unscreened Fe $3d^4$ final states and peak **d** to Fe^{2+} species. The VB of a 5 nm thick Al_2O_3 ALD film deposited on RuO_2 is shown as comparison. (b) VB spectra of sample B and (c) sample C exposed to 10 TMA pulses.

peak **a** and satellite **s**, whereas peaks **b** and **c** become broader and peak **d** increases. Comparing the VB spectrum of a 5 nm thick Al_2O_3 ALD layer on RuO_2 with that of Fe_2O_3 after 1 TMA pulse (Figure 1a), it is clear that the presence of Al−O bonds cannot be responsible for the decrease of features **a** and **s** or for the increase of peak **d**, but it might have an effect on the changes of peaks **b** and **c**. The changes observed after 1 TMA pulse are further enhanced after additional five TMA pulses (six in total), with the exception of peak **d**, the intensity of which stays constant.

Finally, the VB peaks do not change visibly after additional TMA pulses up to a total of 10. Core level spectra of Al 2p indicate that the surface is passivated after six TMA pulses and further TMA pulses do not increase the Al 2p intensity appreciably (Supporting Information SI1), as expected for the self-limiting ALD reactions with TMA. Similarly, the intensity of the Fe 3p peak does not decrease further between the sixth and the tenth TMA pulses. Its intensity attenuation indicates a complete coverage of the surface with a 0.25 nm film after ten TMA pulses (Supporting Information SI2), that is, only one layer is produced in our experiment.

It seems that TMA reacts with the oxygen in hematite and Al−O bonds are produced without oxygen diffusion from the substrate and with a partial removal of methyl groups during chemisorption on the substrate. Further exposure of the sample to TMA does not produce any spectroscopic change because TMA does not react with the adsorbed methyl groups, as confirmed by previous in situ ALD studies of the TMA−water process.[21] The magnitude of spectroscopic changes after each TMA pulse and the amount of deposited Al depended on the hematite temperature during exposure (Supporting Information SI2).

Sample B was characterized before and after 10 TMA pulses at 150 °C. It showed a VB modification similar to that of sample A (Figure 1b), although the initial intensity of peak **d** in sample B was much lower than that of sample A. Differently from the ALD films, sample C had only a negligible intensity of peak **d** even after the TMA pulses at 150 °C, suggesting that the increase of peak **d** is due to some specific property of the hematite ALD films. The appearance and change of this feature is therefore dependent on the quality or morphology of hematite.

The O 1s-XAS spectrum of sample A before TMA treatment shows typical features of hematite (Figure 2).[11,22] Similarly to

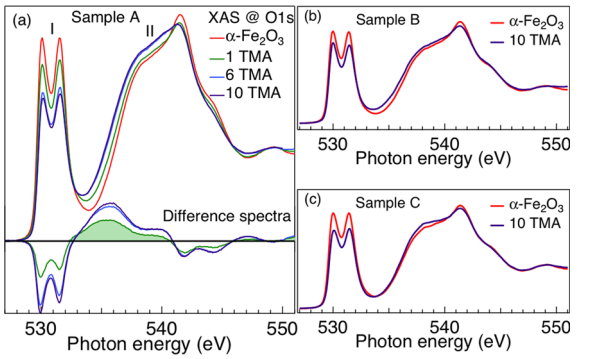

Figure 2. (a) X-ray absorption spectra (XAS) at O 1s edge of sample A before and after, respectively, 1, 6, and 10 TMA pulses. The intensity decrease of feature I is due to the decrease of O 2p−Fe 3d hybridization and the increase of feature II to the increase of O 2p−Fe 4s4p hybridization. Difference spectra show which states are added in the conduction band by the reaction of TMA with Fe_2O_3. (b) XAS of sample B and (c) C before and after 10 TMA pulses.

the VB spectrum, the XAS spectrum is modified after the TMA pulses. The main changes are observed for the intensity of the double peak between 530 and 532 eV (feature I in Figure 2a), and the shape of the broad feature between 535 and 546 eV (feature II in Figure 2a). The double peak I decreases in intensity after the TMA pulses but its shape does not change appreciably. Different Fe oxides are characterized by different shapes of feature I. This has an excitonic character and is assigned to O 2p−Fe 3d hybridized species delivering sharp t_{2g} and e_g states separated by the ligand field,[22] which is different

dx.doi.org/10.1021/jz501751w | J. Phys. Chem. Lett. 2014, 5, 3582−3587

for the various Fe_2O_3 polymorphs and for Fe_3O_4.[22] The persistence of the same shape of feature I indicates that the TMA covered α-Fe_2O_3 has still the same distribution of t_{2g} and e_g states; that is, it is still hematite.

The lower intensity of feature I after the TMA pulses indicates that the O 2p−Fe 3d hybridized states are partially removed, as already observed in the VB. The shape variation of feature II, usually attributed to mixed O 2p−Fe 4s4p states,[11,22] denotes that the distribution of these hybridized states changes after the TMA pulses, as evidenced by the difference spectra in Figure 2a. Samples B and C show a similar evolution of the XAS (Figure 2b and c), demonstrating that the observed changes are connected with the exposure of hematite to TMA. The intensity of the changes, however, is smaller for samples B and C (but comparable between them) compared to sample A. This is due to the different substrate temperatures used during the TMA exposure (Supporting Information SI2). There are other small details in the XAS, like the intensity at 533.5 eV and the small shoulder at 544 eV, that do not vary in sample C. These, together with peak **d** in the VB should be attributed to the different chemical nature of the hematite samples.

From the results shown above, the common feature of the three samples after TMA exposures is the change of O 2p−Fe 3d and O 2p−Fe 4s4p hybridizations. The origin of the modified O 2p−Fe 3d and O 2p−Fe 4s4p hybridizations can be related to the reactions between TMA and Fe_2O_3, which result in the removal of methyl ligands and the formation of chemical bonds between Al and the oxygen atoms from hematite. The ligands are formally negatively charged $(CH_3)^-$ while attached to Al. However, when they leave Al and migrate to O, they become positively charged $(CH_3)^+$ and transfer two electrons to the hematite.[23] After this first migration step, the CH_3 groups can be completely removed from the surface by reacting further to form volatile molecules such as C_2H_4 and C_2H_6, which desorb. This is one of the reactions that Klejna and Elliott[23] proposed to explain the cleanup of GaAs native oxide with TMA and that we adopt for hematite, although in our system it may compete with other processes that are specific for the TMA/Fe_2O_3 interface. Liu et al.[24] observed that methyl radicals may react with hematite substrates and, depending on the exposed surface, may reduce Fe^{3+} into Fe^{2+}. Moreover, the interfacial reduction of hematite needs the simultaneous presence of an oxygen dangling-bond and a reducible Fe^{3+}. Therefore, the actual reactions depend on the exposed surface and can be different for differently prepared hematite samples, as we have observed.

The extra electrons due to the methyl removal can be included in hematite as small polarons, that is, inducing a small (local) structural distortion,[4] but maintaining the formal oxidation state of Fe^{3+}. Polarons can be self-trapped by the structural distortion or travel inside the substrate, although with a large effective mass.[6] Peng and Lany[6] attributed the tendency to form electron self-trapped states in hematite to the high density of Fe 3d-derived t_{2g} states just above the conduction band minimum (CBM). On the other hand, the structural distortion associated with the formation of polarons may cause the variations in the hybridization of O 2p with Fe 3d and Fe 4s4p states.[11,22] As observed, the density of t_{2g} (and e_g) states next to the CBM decreases after the TMA treatment. Following the predictions of Peng and Lany, we expect that the decreased intensity of CBM states reduces the tendency of electrons to self-trap, lowering their m_{eff} and letting them spread over many unit cells. A similar electron enrichment was recently discussed by Kronawitter et al.[25] in ALD TiO_2 films deposited on Fe_2O_3. However, they used XAS on ex-situ samples and, therefore, assigned the electron enrichment to macroscopic system properties. Instead, here, we show that the ALD reactions produce the modification of the hematite electronic properties using in-situ measurements.

The presence of extra electrons in hematite could apparently be related with the increase of peak **d** in the VB spectra of samples A and B after exposure to TMA. Nevertheless, the absence of such a strong increase in sample C indicates that the intensity of peak **d** depends on the nature of hematite and should be further analyzed. Feature **d** in sample A is due to a large peak starting at 0.5 eV below the Fermi level and extending to about 1.8 eV (d_1 in Figure 3a). Its energy position

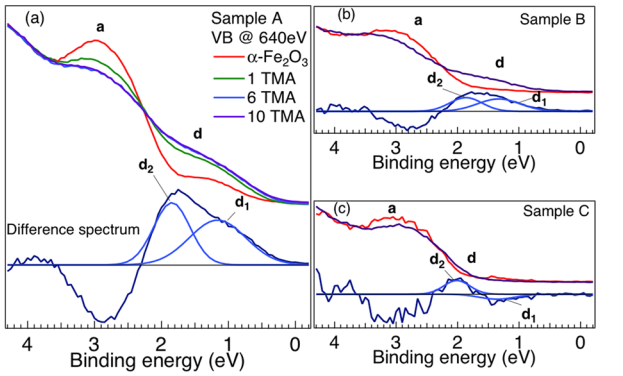

Figure 3. Detail of the VB of samples A−C for peaks **a** and **d**. Difference spectra between the spectra before and after TMA modification show two main contributions (d_1 and d_2). d_1 is assigned to Fe^{2+} species, and d_2 to electron enrichment.

is very similar to that observed by Gajda-Schrantz et al.,[20] who attributed it to Fe^{2+} species. Nevertheless, the intensity increase of this feature after the TMA exposure starts already at about 2.3 eV (d_2). In the difference spectra the two components can be clearly observed (Figure 3a). The VB spectra of sample B after the TMA exposure show also the increase of both d_1 and d_2 components (Figure 3b). In sample C, instead, there is only an increase of peak d_2 (Figure 3c). From the comparison of the three spectra, the difference of about 0.2 eV in binding energy between samples A and B on the one side, and sample C on the other, is clear. This is due to the different substrates used to grow hematite (Si or FTO), which deliver a different band alignment due to the different work functions of Si and FTO. Finally, we can link the changes of peak d_2 to the polaronic electron transfer, and the changes of peak d_1 to the reactions leading to the reduction of Fe^{3+} to Fe^{2+}.

The different behavior of the three samples after the TMA pulses can be attributed to their different morphology. This is evident from the XRD patterns (Supporting Information SI3): sample C shows prevalent (110) and (300) directions for the hematite growth, which occurs in the form of oriented hematite nanocolumns, whereas the ALD films have multifaceted surfaces for which the reduction of hematite by TMA is more probable.[24] In the case of sample C, most of the exposed facets are perpendicular to the (110) direction (sidewall facets).

The differences in the VB are equivalent to those in the XAS, so that the decrease of feature **I** and the increase of the peak at 539 eV of feature **II** are due to electron doping and the consequent modification of hybridization, whereas the increase at 535.5 eV is related to Fe^{2+}. Fe 2p-XAS spectra showed

dx.doi.org/10.1021/jz501751w | J. Phys. Chem. Lett. 2014, 5, 3582−3587

indeed the occurrence of Fe^{3+} to Fe^{2+} reduction in samples A and B and not in sample C (see Supporting Information SI4).[26−28]

The main effects of TMA on hematite is to change the hybridization properties of the O−Fe bond and to trigger the presence of Fe^{2+} species in samples A and B. These changes can have a beneficial effect on the photoresponse enhancement of the TMA modified samples.[29] To verify this, we obtained the photocurrent response of samples B and C after 10 TMA pulses and we compared it with that of pristine samples (Figure 4).

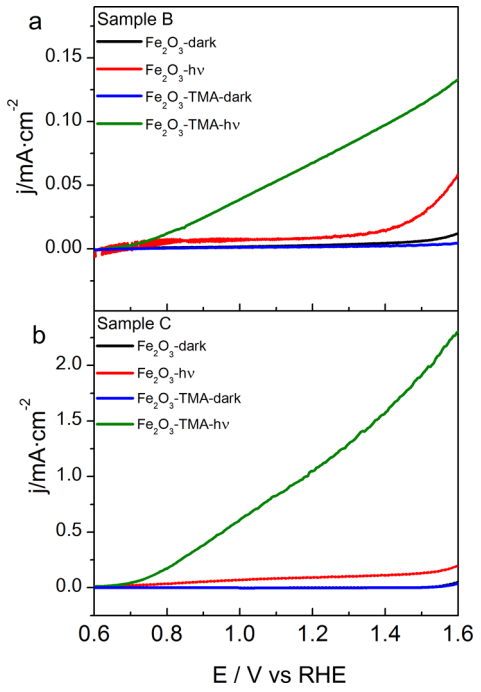

Figure 4. Photoelectrochemical characterization of samples B (a) and C (b) in 1 M NaOH electrolyte before and after 10 TMA pulses, in the dark and under illumination. The illumination source for sample B was a tungsten lamp (40 mW/cm^2), and for sample C was a Xe arc lamp with irradiance of 400 mW/cm^2 equipped with a visual band-pass filter.

These experiments were done in 1 M NaOH, although it should be mentioned that the illumination conditions employed for both samples were different (details in Supporting Information SI5). In both cases, the modification with TMA led to a dramatic improvement of the photocurrent. Concretely, the photocurrent at 1.23 V (vs RHE) for sample B increased by a factor of 8, and for sample C by a factor of 11. From the comparison, we can observe that the Fe^{2+} species (only present in sample B) do not seem to have a specific positive effect on the photoresponse of hematite modified with TMA.

Therefore, we can assign the enhancement of the photoresponse unequivocally to the changed Fe−O bond properties. The electronic changes produced by the reaction with TMA are probably localized next to the interface; however, this is of the same order of magnitude as the diffusion length of holes, that is, about 4 nm. Our results do not preclude that surface passivation could also be occurring, thus contributing to the photocurrent enhancement.[9,30] However, we do not have any experimental evidence for it, and more work is in progress to address this question.

Le Formal et al.[9] also observed an improvement in the PEC response after depositing one ALD layer of Al_2O_3 on hematite photoanodes, although it was more modest than that observed by us. We can therefore link the spectroscopic changes of our samples to a more general behavior of hematite after the ALD of a thin Al_2O_3 film, associated with a modified covalency of the Fe−O bond next to the interface.

Our results agree with many other works in the literature regarding the optimization of hematite photoelectrodes with various methods, although the comparison of spectroscopy and electrochemical behavior was not always present in these works. Postdeposition treatments increase the efficiency of hematite, for example, annealing at 500 to 800 °C,[11−13] nanostructuring,[11,31] or doping.[11,13,32,33]

Herrmann-Geppert et al. observed a decrease of peak **a** in the VB of hematite after plasma treatment[34] and an increased photoresponse of Fe_2O_3 as in our case. Al-doped Fe_2O_3 photoanodes evidenced also a photoresponse enhancement that was assigned to a contraction of the crystal lattice, inducing a conductivity improvement compared to undoped samples.[35] Kronawitter et al.[11] observed that annealing Fe_2O_3 films deposited on FTO substrates at 800 °C decreased the O 2p−Fe 3d hybridization, causing an increase of photoresponse. Sivula et al.[12] observed that mesoporous Fe_2O_3 photoanodes had enhanced photocurrent response after sintering at 800 °C and assigned it to a change in the Fe−O bond length. All such different modifications of pristine hematite induced similar PEC improvements to those observed by us and could be related to the modification of the Fe−O covalent bond.

The ALD of Al_2O_3 based on TMA produces modifications in the electronic properties of α-Fe_2O_3 favoring the improvement of its photoelectrochemical behavior. Reactions between TMA and α-Fe_2O_3 induce electron donation to the substrate in the form of small polarons and modify the covalent character of the Fe−O bonds. These Fe_2O_3 surface modifications probably allow for an enhanced charge carrier transport next to the interface and explain the photoelectrochemical enhancement observed in hematite photoanodes. We believe that this work contributes to the understanding of some of the mechanisms underlying the enhancement of hematite photoanodes by means of surface modification and that it may open new avenues for further improving their performance in the context of water splitting.

■ ASSOCIATED CONTENT

Supporting Information

Experimental section (SI0). Al 2p and Fe 3p spectra and thickness calculation (SI1). VB variations at different substrate temperatures (SI2). XRD characterization of samples A−C (SI3). Comparison of Fe 2p-XAS of samples A−C (SI4). Electrochemical characterization of samples B and C (SI5). This material is available free of charge via the Internet at http://pubs.acs.org.

■ AUTHOR INFORMATION

Corresponding Author

*E-mail: tallamas@tu-cottbus.de.

Author Contributions

The manuscript was written through contributions of all authors. All authors have given approval to the final version of the manuscript.

Notes

The authors declare no competing financial interest.

■ ACKNOWLEDGMENTS

Authors thank S. Elliott for fruitful discussions and M. Richter and T. Arroval for experimental support. Funding from the German Research Foundation (DFG) with the project SCHM 745/31-1, the German Ministry for Education and Research (BMBF) with the grant 03IN2 V4A, the Spanish Ministry of Economy and Competitiveness (MINECO) through the project MAT2012-37676 (FONDOS FEDER), the Finnish Centre of Excellence in Atomic Layer Deposition (CoE ALD), and the Estonian Research Agency (ETAg) with the project PUT170 is acknowledged. D.C. is grateful to MINECO for the award of an FPI grant.

■ REFERENCES

(1) Chen, J.; Xu, L.; Li, W.; Gou, X. α-Fe_2O_3 Nanotubes in Gas Sensor and Lithium-Ion Battery Applications. *Adv. Mater.* **2005**, *17*, 582−586.

(2) Cheng, K.; He, Y. P.; Miao, Y. M.; Zou, B. S.; Wang, Y. G.; Wang, T. H.; Zhang, X. T.; Du, Z. L. Quantum Size Effect on Surface Photovoltage Spectra: α-Fe_2O_3 Nanocrystals on the Surface of Monodispersed Silica Microsphere. *J. Phys. Chem. B* **2006**, *110*, 7259−7264.

(3) Sivula, K.; Le Formal, F.; Graetzel, M. Solar Water Splitting: Progress Using Hematite (α-Fe_2O_3) Photoelectrodes. *Chem. Sus. Chem.* **2011**, *4*, 432−449.

(4) Rosso, K. M.; Dupuis, M. Electron Transfer in Environmental Systems: a Frontier for Theoretical Chemistry. *Theor. Chem. Acc.* **2006**, *116*, 124−136.

(5) Liao, P.; Toroker, M. C.; Carter, E. A. Electron Transport in Pure and Doped Hematite. *Nano Lett.* **2011**, *11*, 1775−1781.

(6) Peng, H.; Lany, S. Semiconducting Transition-Metal Oxides Based on d^5 Cations: Theory for MnO and Fe_2O_3. *Phys. Rev. B* **2012**, *85*, 201202.

(7) Klahr, B. M.; Martinson, A. B. F.; Hamann, T. W. Photoelectrochemical Investigation of Ultrathin Film Iron Oxide Solar Cells Prepared by Atomic Layer Deposition. *Langmuir* **2011**, *27*, 461−468.

(8) Klahr, B.; Gimenez, S.; Fabregat-Santiago, F.; Hamann, T.; Bisquert, J. Water Oxidation at Hematite Photoelectrodes: The Role of Surface States. *J. Am. Chem. Soc.* **2012**, *134*, 4294−4302.

(9) Le Formal, F.; Tetreault, N.; Cornuz, M.; Moehl, T.; Grätzel, M.; Sivula, K. Passivating Surface States on Water Splitting Hematite Photoanodes with Alumina Overlayers. *Chem. Sci.* **2011**, *2*, 737−743.

(10) Le Formal, F.; Sivula, K.; Grätzel, M. The Transient Photocurrent and Photovoltage Behavior of a Hematite Photoanode under Working Conditions and the Influence of Surface Treatments. *J. Phys. Chem. C* **2012**, *116*, 26707−26720.

(11) Kronawitter, C. X.; Zegkinoglou, I.; Rogero, C.; Guo, J. H.; Mao, S. S.; Himpsel, F. J.; Vayssieres, L. On the Interfacial Electronic Structure Origin of Efficiency Enhancement in Hematite Photoanodes. *J. Phys. Chem. C* **2012**, *116*, 22780−22785.

(12) Sivula, K.; Zboril, R.; Le Formal, F.; Robert, R.; Weidenkaff, A.; Tucek, J.; Frydrych, J.; Graetzel, M. Photoelectrochemical Water Splitting with Mesoporous Hematite Prepared by a Solution-Based Colloidal Approach. *J. Am. Chem. Soc.* **2010**, *132*, 7436−7444.

(13) Zandi, O.; Hamann, T. W. Enhanced Water Splitting Efficiency Through Selective Surface State Removal. *J. Phys. Chem. Lett.* **2014**, *5*, 1522−1526.

(14) Tallarida, M.; Kukli, K.; Michling, M.; Ritala, M.; Leskelä, M.; Schmeisser, D. Substrate Reactivity Effects in the Atomic Layer Deposition of Aluminum Oxide from Trimethylaluminum on Ruthenium. *Chem. Mater.* **2011**, *23*, 3159−3168.

(15) Tallarida, M.; Adelmann, C.; Delabie, A.; Van Elshocht, S.; Caymax, M.; Schmeisser, D. Surface Chemistry and Fermi Level Movement During the Self-Cleaning of GaAs by Trimethyl-Aluminum. *Appl. Phys. Lett.* **2011**, *99*, 042906.

(16) Kim, C. Y.; Bedzyk, M.; Nelson, E.; Woicik, J.; Berman, L. Site-Specific Valence-Band Photoemission Study of α-Fe_2O_3. *Phys. Rev. B* **2002**, *66*, 085115.

(17) Liao, P.; Carter, E. A. Testing Variations of the GW Approximation on Strongly Correlated Transition Metal Oxides: Hematite (α-Fe_2O_3) as a Benchmark. *Phys. Chem. Chem. Phys.* **2011**, *13*, 15189−15199.

(18) Fujimori, A.; Saeki, M.; Kimizuka, N.; Taniguchi, M.; Suga, S. Photoemission Satellites and Electronic Structure of Fe_2O_3. *Phys. Rev. B* **1986**, *34*, 7318−7328.

(19) Fujii, T.; de Groot, F.; Sawatzky, G.; Voogt, F.; Hibma, T.; Okada, K. In Situ XPS Analysis of Various Iron Oxide Films Grown by NO_2-Assisted Molecular-Beam Epitaxy. *Phys. Rev. B* **1999**, *59*, 3195−3202.

(20) Gajda-Schrantz, K.; Tymen, S.; Boudoire, F.; Toth, R.; Bora, D. K.; Calvet, W.; Grätzel, M.; Constable, E. C.; Braun, A. Formation of an Electron Hole Doped Film in the α-Fe_2O_3 Photoanode Upon Electrochemical Oxidation. *Phys. Chem. Chem. Phys.* **2013**, *15*, 1443−1451.

(21) Juppo, M.; Rahtu, A.; Ritala, M.; Leskelä, M. In Situ Mass Spectrometry Study on Surface Reactions in Atomic Layer Deposition of Al_2O_3 Thin Films from Trimethylaluminum and Water. *Langmuir* **2000**, *16*, 4034−4039.

(22) de Groot, F.; Grioni, M.; Fuggle, J. C.; Ghijsen, J.; Sawatzky, G. A.; Petersen, H. Oxygen 1s X-ray-absorption Edges of Transition-Metal Oxides. *Phys. Rev. B* **1989**, *40*, 5715−5720.

(23) Klejna, S.; Elliott, S. D. First-Principles Modeling of the "Clean-Up" of Native Oxides During Atomic Layer Deposition onto III-V Substrates. *J. Phys. Chem. C* **2012**, *116*, 643−654.

(24) Liu, L.; Quezada, B. R.; Stair, P. C. Adsorption, Desorption, and Reaction of Methyl Radicals on Surface Terminations of α-Fe_2O_3. *J. Phys. Chem. C* **2010**, *114*, 17105−17111.

(25) Kronawitter, C. X.; Bakke, J. R.; Wheeler, D. A.; Wang, W.-C.; Chang, C.; Antoun, B. R.; Zhang, J. Z.; Guo, J.; Bent, S. F.; Mao, S. S.; et al. Electron Enrichment in 3d Transition Metal Oxide Hetero-Nanostructures. *Nano Lett.* **2011**, *11*, 3855−3861.

(26) Crocombette, J.; Pollak, M.; Jollet, F.; Thromat, N.; Gautier-Soyer, M. *Phys. Rev. B* **1995**, *52*, 3143−3150.

(27) Miedema, P. S.; de Groot, F. M. F. The Iron L Edges: Fe 2p X-ray Absorption and Electron Energy Loss Spectroscopy. *J. Electron Spectrosc. Relat. Phenom.* **2013**, *187*, 32−48.

(28) de Groot, F. Multiplet Effects in X-ray Spectroscopy. *Coord. Chem. Rev.* **2005**, *249*, 31−63.

(29) Ling, Y.; Wang, G.; Reddy, J.; Wang, C.; Zhang, J. Z.; Li, Y. The Influence of Oxygen Content on the Thermal Activation of Hematite Nanowires. *Angew. Chem., Int. Ed.* **2012**, *51*, 4074−4079.

(30) Yang, X.; Liu, R.; Du, C.; Dai, P.; Zheng, Z.; Wang, D. Improving Hematite-Based Photoelectrochemical Water Splitting with Ultrathin TiO_2 by Atomic Layer Deposition. *ACS Appl. Mater. Interfaces* **2014**, *6*, 12005−12011.

(31) Gemmer, J.; Hinrichsen, Y.; Abel, A.; Bachmann, J. Systematic Catalytic Current Enhancement for the Oxidation of Water at Nanostructured Iron(III) Oxide Electrodes. *J. Catal.* **2012**, *290*, 220−224.

(32) Cesar, I.; Sivula, K.; Kay, A.; Zboril, R.; Grätzel, M. Influence of Feature Size, Film Thickness, and Silicon Doping on the Performance of Nanostructured Hematite Photoanodes for Solar Water Splitting. *J. Phys. Chem. C* **2008**, *113*, 772−782.

(33) Shen, S.; Kronawitter, C. X.; Jiang, J.; Mao, S. S.; Guo, L. Surface Tuning for Promoted Charge Transfer in Hematite Nanorod Arrays as Water-Splitting Photoanodes. *Nano Res.* **2012**, *5*, 327−336.

(34) Herrmann-Geppert, I.; Bogdanoff, P.; Radnik, J.; Fengler, S.; Dittrich, T.; Fiechter, S. Surface Aspects of Sol-Gel Derived Hematite Films for the Photoelectrochemical Oxidation of Water. *Phys. Chem. Chem. Phys.* **2013**, *15*, 1389−1398.

(35) Kleiman-Shwarsctein, A.; Huda, M. N.; Walsh, A.; Yan, Y.; Stucky, G. D.; Hu, Y.-S.; Al-Jassim, M. M.; McFarland, E. W.

Electrodeposited Aluminum-Doped α-Fe_2O_3 Photoelectrodes: Experiment and Theory. *Chem. Mater.* **2010**, *22*, 510−517.